NH_3-promoted hydrolysis of NO_2 induces explosive growth in HONO

Wanyun Xu[1], Ye Kuang[2,*], Chunsheng Zhao[3], Jiangchuan Tao[2], Gang Zhao[3], Yuxuan Bian[4], Wen Yang[5], Yingli Yu[3], Chuanyang Shen[3], Linlin Liang[1], Gen Zhang[1], Weili Lin[6], Xiaobin Xu[1]

[1] State Key Laboratory of Severe Weather, Key Laboratory for Atmospheric Chemistry, Institute of Atmospheric Composition, Chinese Academy of Meteorological Sciences, Beijing, 100081, China.

2 Institute for Environmental and Climate Research, Jinan University, Guangzhou, China.

[3] Department of Atmospheric and Oceanic Sciences, School of Physics, Peking University, Beijing, China

[4] State Key Laboratory of Severe Weather, Chinese Academy of Meteorological Sciences, Beijing, 100081, China

[5] State Key Laboratory of Environmental Criteria and Risk Assessment, Chinese Research Academy of Environmental Sciences, Beijing, 100081, China

[6] College of Life and Environmental Sciences, Minzu University of China, Beijing, 100081, China

Corresponding author: Ye Kuang (kuangye@jnu.edu.cn)

Table S1. AOD assumptions for the TUV model calculations

RH (%)	AOD
40-55	0.6
55-70	0.8
70-80	1
80-90	1.5
90-97	2
97-100	2.5

The above assumptions were made based on the change in dry state scattering coefficient (σ_{sp}), f(RH) and RH between 11:30 to 13:30 on the 14. Nov. and the observed MODIS AOD at 13:30, we made AOD assumptions varying with RH.

The MODIS AOD, σ_{sp} and RH at 13:30 on the 14. Nov. was 0.6, 1200 Mm^{-1} and 43%, respectively. The σ_{sp} and RH at 11:30 was 800 Mm^{-1} and 85%. Hence, the AOD at 11:30 was estimated to be 1.44 (0.6×1200/800).

Table S2. The trace gas concentrations, liquid water content, mean diameter and temperature used to calculate the heterogeneous sulfate production

Date	Time (LT)	SO_2 (ppb)	H_2O_2 (ppb)	NO_2 (ppb)	O_3 (ppb)	LWC (g m^{-3})	D_p (μm)	T (K)
4th Nov	9:00	0.18	0.26	45.3	1.53	0.3	7.00	277.8
	10:00	0.17	0.29	48.8	1.56	0.3	7.00	278.4
	11:00	0.28	0.34	49.9	1.78	0.3	7.00	278.7
5th Nov.	10:00	0.16	0.19	44.6	2.90	0.3	7.00	278.8
	11:00	0.39	0.21	44.0	3.39	0.3	7.00	279.6
	12:00	1.19	0.30	45.1	5.72	0.3	7.00	281.3
11th Nov.	7:00	0.40	0.52	30.7	1.41	3.4 e^{-4}	1.22	271.2
	8:00	0.44	0.71	33.0	1.53	2.1e^{-4}	0.73	272.3
	9:00	1.61	0.89	32.7	1.83	7.8e^{-5}	0.65	274.8
14th Nov.	11:00	1.27	0.32	41.6	1.52	0.01	0.90	278.1

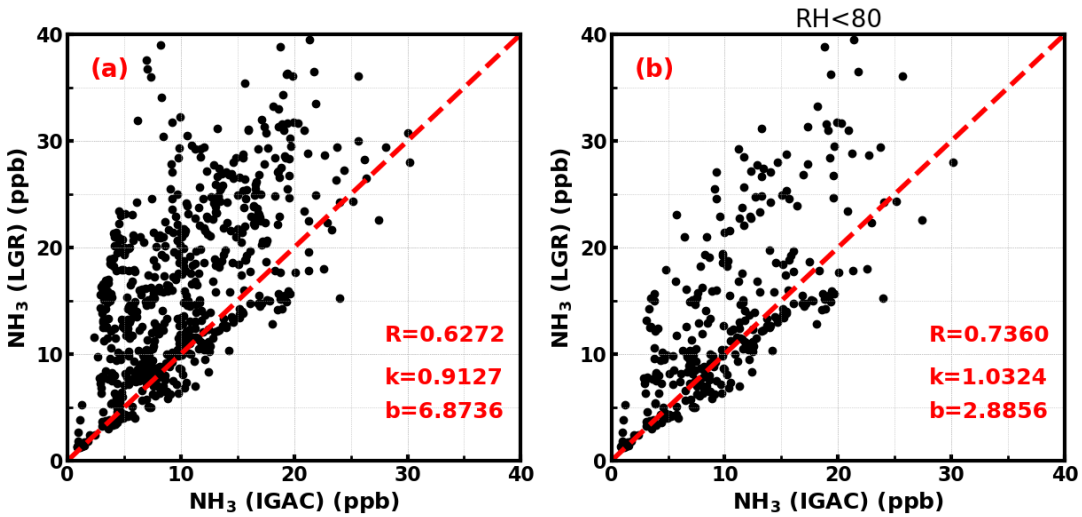

Figure S1 Comparison between $NH_{3,IGAC}$ and $NH_{3,LGR}$ using a) all measurement data and b) data associated with RH<80.

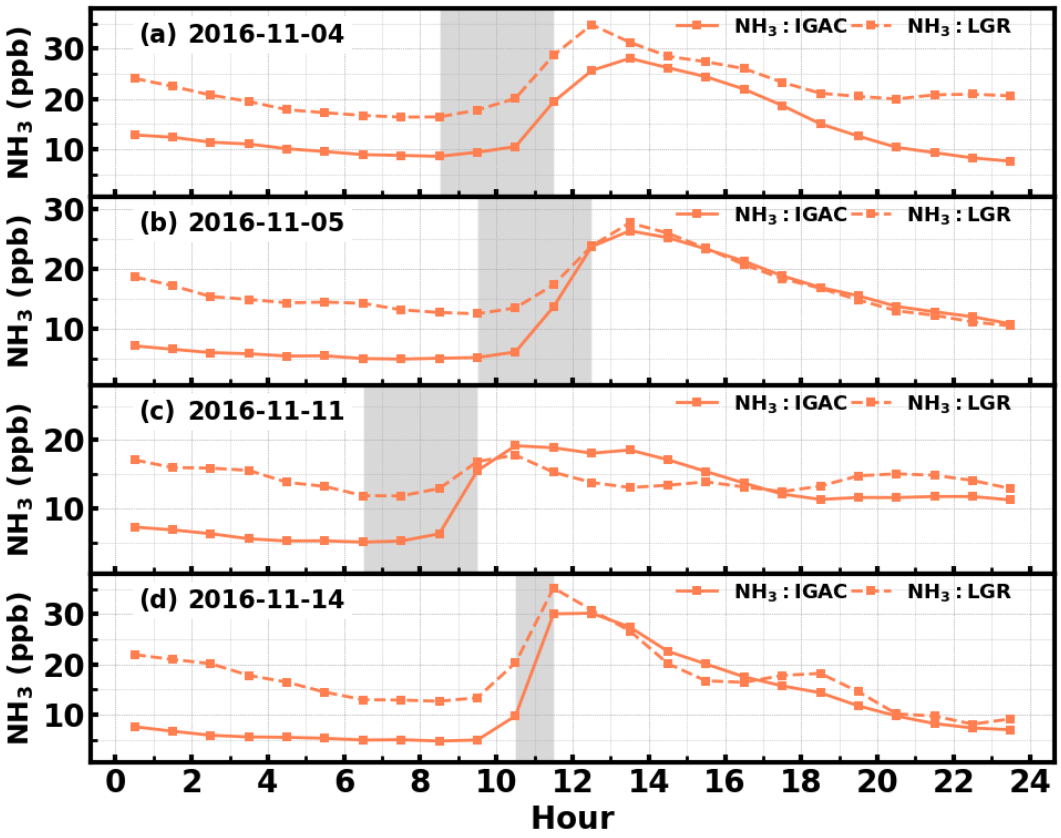

Figure S2 Time series of $NH_{3,IGAC}$ (solid) and $NH_{3,LGR}$ (dashed) during a) 4th Nov., b) 5th Nov., c) 11th Nov. 2016 and d) 14th Nov. 2016. Gray shaded areas represents periods of rapid increase of HONO.

a) 2016-11-04–2016-11-05

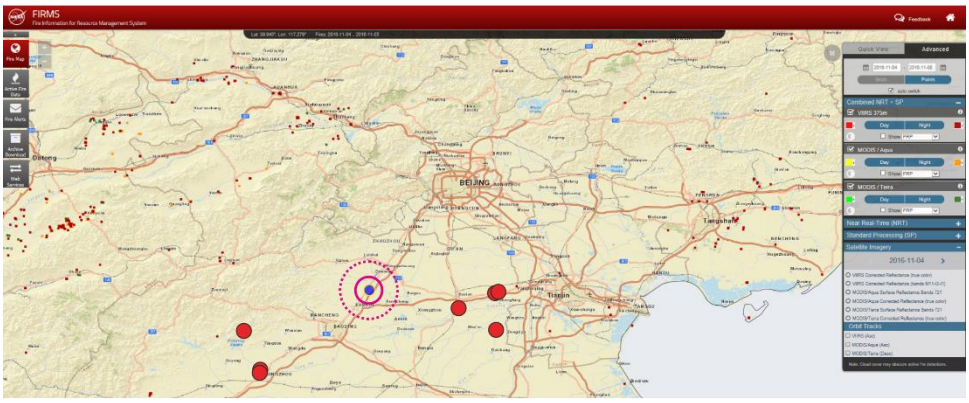

b) 2016-11-11

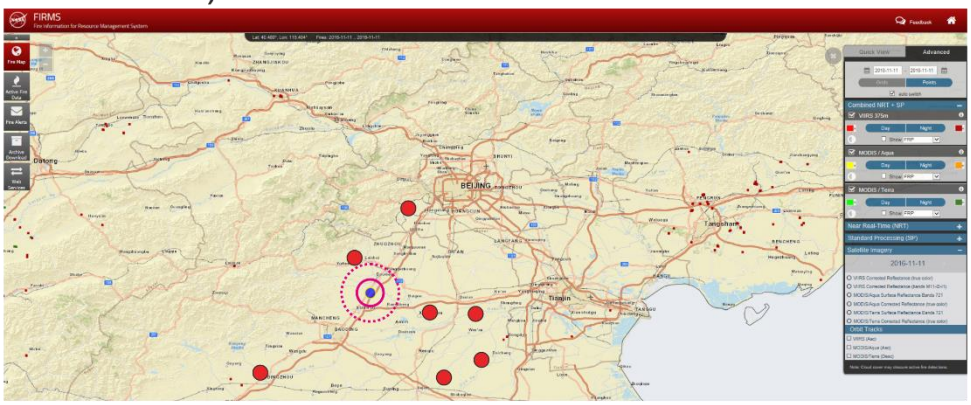

c) 2016-11-14

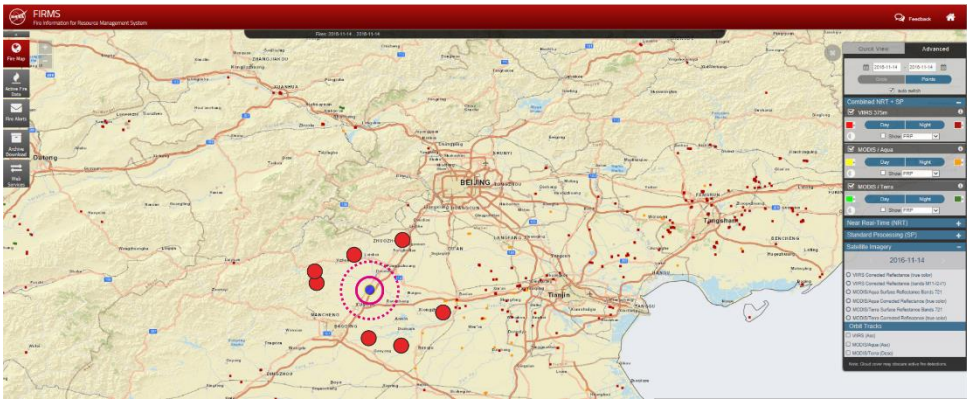

Figure S3. Fire spots maps (large red dots: fire spots closest to the station, bright and red dots: VIIRS, yellow and orange dots: MODIS Aqua, bright and dark green dots: MODIS Terra) produced by NASA's Web Fire Mapper (https://firms.modaps. eosdis. nasa.gov/firemap/), respectively for the 4th-5th, 11th and 14th Nov. 2016. The blue dot shows the location of the Gucheng site, while the pink solid and dashed line circles respectively cover areas within 10 and 20 km distance.

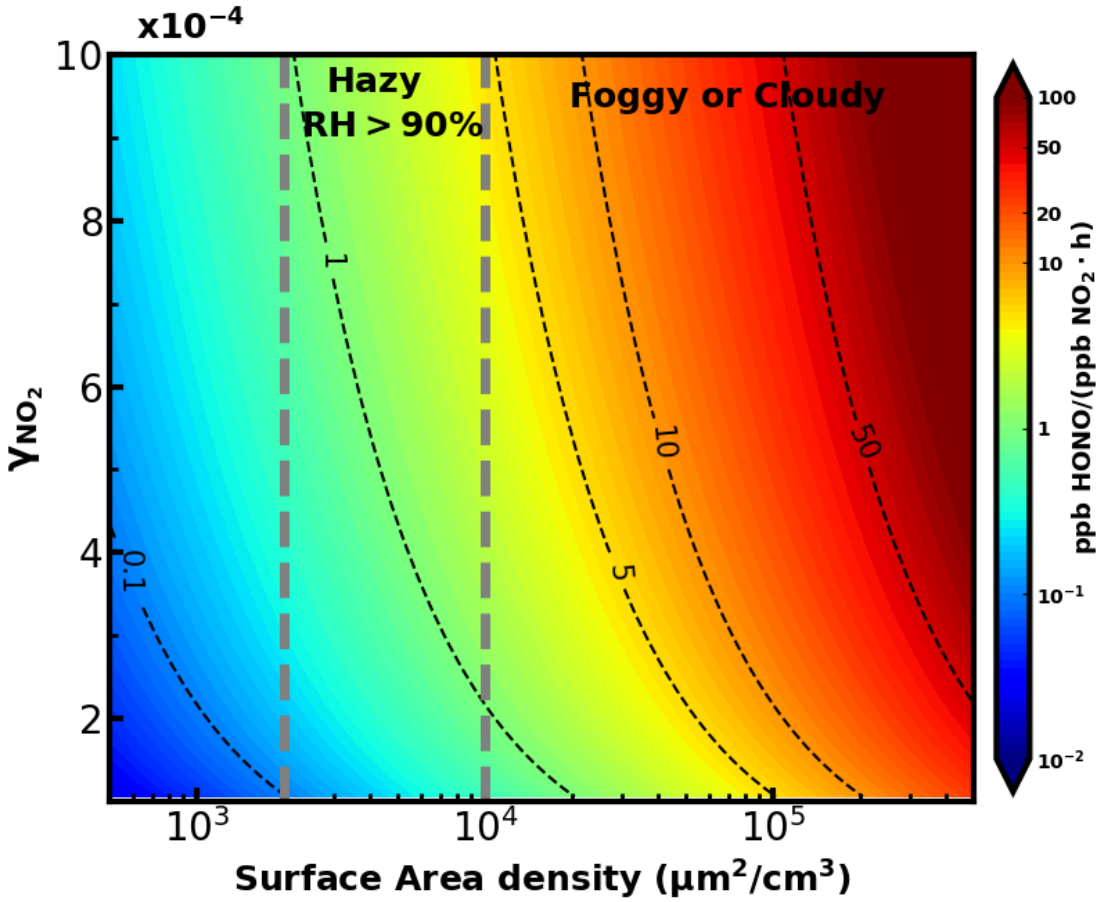

Figure S4. The production rate of HONO under different conditions and with different values of reactive NO_2 uptake coefficients (γ_{NO_2}), the γ_{NO_2} range is from Li et al. (2018). The surface area density range of fog is calculated based on the fog droplet size distribution measured on the North China Plain (Shen et al., 2018).

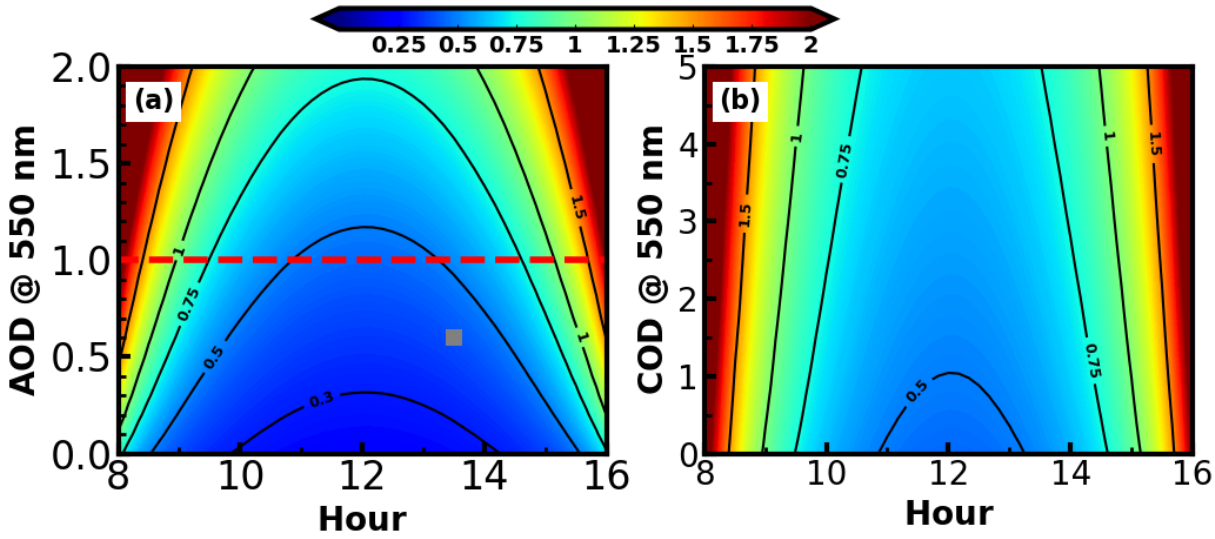

Figure S5. **(a)** Diurnal variations of lifetime of HONO under different aerosol optical depth (AOD) conditions. Gray solid marker represents the AOD position from MODIS Aqua on the 14th Nov. 2016 (about 13:30); **(b)** Diurnal variations of lifetime of HONO under different cloud optical depth (COD) conditions, with an AOD of 1.

Indirect oxidation of S(IV) by HONO:

$HONO + h\nu \rightarrow NO + OH$ (RS1)

$OH + HSO_3^- + O_2 \rightarrow HSO_4^- + HO_2$ (RS2)

$OH + RH + O_2 \rightarrow RO_x + HO_2$ (RS3)

$HO_2 + NO \rightarrow NO_2 + OH$ (RS4)

$HO_2 + HO_2 \rightarrow H_2O_2 + O_2$ (RS5)

$HSO_3^- + H_2O_2 \rightarrow HSO_4^- + H_2O$ (RS6)

Reference

Li, L., Hoffmann, M. R., and Colussi, A. J.: Role of Nitrogen Dioxide in the Production of Sulfate during Chinese Haze-Aerosol Episodes, Environmental science & technology, 10.1021/acs.est.7b05222, 2018.

Shen, C., Zhao, C., Ma, N., Tao, J., Zhao, G., Yu, Y., and Kuang, Y.: Method to Estimate Water Vapor Supersaturation in the Ambient Activation Process Using Aerosol and Droplet Measurement Data, Journal of Geophysical Research: Atmospheres, 123, 10606-10619, doi:10.1029/2018JD028315, 2018.